

ORIGINAL ARTICLE

# Disruption of *Abi1/Hssh3bp1* expression induces prostatic intraepithelial neoplasia in the conditional *Abi1/Hssh3bp1* KO mice

X Xiong<sup>1,8</sup>, A Chorzalska<sup>1,8</sup>, PM Dubielecka<sup>1,9</sup>, JR White<sup>2</sup>, Y Vedvyas<sup>1</sup>, CV Hedvat<sup>3</sup>, A Haimovitz-Friedman<sup>4</sup>, JA Koutcher<sup>5</sup>, J Reimand<sup>6</sup>, GD Bader<sup>6</sup>, JA Sawicki<sup>7</sup> and L Kotula<sup>1</sup>

Prostate cancer is one of the leading causes of cancer-related deaths in the United States and a leading diagnosed non-skin cancer in American men. Genetic mutations underlying prostate tumorigenesis include alterations of tumor suppressor genes. We tested the tumor suppressor hypothesis for *ABI1/hSSH3BP1* by searching for gene mutations in primary prostate tumors from patients, and by analyzing the consequences of prostate-specific disruption of the mouse *Abi1/Hssh3bp1* ortholog. We sequenced the *ABI1/hSSH3BP1* gene and identified recurring mutations in 6 out of 35 prostate tumors. Moreover, complementation and anchorage-independent growth, proliferation, cellular adhesion and xenograft assays using the LNCaP cell line, which contains a loss-of-function *Abi1* mutation, and a stably expressed wild-type or mutated *ABI* gene, were consistent with the tumor suppressor hypothesis. To test the hypothesis further, we disrupted the gene in the mouse prostate by breeding the *Abi1* floxed strain with the probasin promoter-driven Cre recombinase strain. Histopathological evaluation of mice indicated development of prostatic intraepithelial neoplasia (PIN) in *Abi1/Hssh3bp1* knockout mouse as early as the eighth month, but no progression beyond PIN was observed in mice as old as 12 months. Observed decreased levels of E-cadherin,  $\beta$ -catenin and WAVE2 in mouse prostate suggest abnormal cellular adhesion as the mechanism underlying PIN development owing to *Abi1* disruption. Analysis of syngeneic cell lines point to the possibility that upregulation of phospho-Akt underlies the enhanced cellular proliferation phenotype of cells lacking *Abi1*. This study provides proof-of-concept for the hypothesis that *Abi1* downregulation has a role in the development of prostate cancer.

*Oncogenesis* (2012) 1, e26; doi:10.1038/oncsis.2012.28; published online 3 September 2012

**Subject Category:** tumour suppression

**Keywords:** *Abi1*; *Hssh3bp1*; prostate cancer; gene mutations; mouse model

## INTRODUCTION

Multiple genes are now known to be involved in prostate tumorigenesis. Evidence for a role of the *ABI1/SSH3BP1* gene (henceforth referred to as *ABI1*) in human cancer, including prostate cancer, is growing. Alterations of *ABI1* and/or its expression have been found in cancer cells originating from diverse human tissues in which *Abi1* was proposed to have either tumor suppressor or oncogenic function depending on tissue origin. For example, progression of leukemia in an experimental setting appears to require the presence of *Abi1*, indicating its potential oncogenic function.<sup>1</sup> Breast cancer cell lines show altered *ABI1* expression, and an increase in *Abi1* expression has been suggested to be a progression marker in breast cancer patients.<sup>2</sup> In contrast, in gastric<sup>3</sup> and prostate<sup>4</sup> cancers, *ABI1* expression is downregulated, suggesting its tumor suppressor function in these tissues.

Cytological studies lend further support to assigning a tumor suppression function to *ABI1* in the prostate. Location of the *ABI1* gene to 10p11.2,<sup>5</sup> a region of chromosome 10p often involved in loss of heterozygosity in prostate cancer, led to subsequent studies demonstrating that loss of *ABI1* expression is associated with 10p loss.<sup>4</sup> Moreover, the prostate tumor cell line, LNCaP, contains an exon 6-skipping mutation in *ABI1*.<sup>4</sup> We further established that, as a result of the loss of phosphotyrosine 213 in exon 6, the *Abi1*-binding site to SH2 domains of *Abl* kinase<sup>6</sup> and the p85 regulatory subunit of PI3 kinase<sup>7</sup> were inactivated. These findings linked *Abi1* to PI-3 kinase function, which is the key pathway dysregulated in prostate cancer.<sup>8</sup>

*Abi1* is the key component of the WAVE2 complex upstream of Arp2/3-dependent actin polymerization.<sup>9–12</sup> WAVE complexes have important roles in a variety of cellular processes, including protrusion formation during cell migration, and the formation of

<sup>1</sup>Laboratory of Cell Signaling, New York Blood Center, New York, NY, USA; <sup>2</sup>Laboratory of Comparative Pathology, Memorial Sloan-Kettering Cancer Center, New York, NY, USA; <sup>3</sup>Department of Pathology, Memorial Sloan-Kettering Cancer Center, New York, NY, USA; <sup>4</sup>Department of Radiation Oncology, Memorial Sloan-Kettering Cancer Center, New York, NY, USA; <sup>5</sup>Department of Medical Physics, Memorial Sloan-Kettering Cancer Center, New York, NY, USA; <sup>6</sup>The Donnelly Center for Cellular and Biomolecular Research, Department of Molecular Genetics, University of Toronto, Toronto, Canada and <sup>7</sup>Lankenau Institute for Medical Research, Wynnewood, PA, USA. Correspondence: Dr L Kotula. Current address: New York State Institute for Basic Research, 1050 Forest Hill Road, Staten Island, NY 10314, USA.

E-mail: lkotula@gmail.com

<sup>8</sup>First co-authorship.

<sup>9</sup>Current address: Signal Transduction Lab, NIH Center of Biomedical Excellence, Boston University School of Medicine, Roger Williams Medical Center, 825 Chalkstone Avenue, Providence, RI 02908, USA.

Received 20 March 2012; revised 10 July 2012; accepted 31 July 2012

adherens junctions, indicating the critical importance of *Abi1* for cell-to-cell adhesion.<sup>13,14</sup> Moreover, loss of the WAVE2 complex component, CYFIP, is found in a variety of epithelial tumors, including the prostate, thus suggesting involvement of dysregulated cellular adhesion as a possible mechanism.<sup>15</sup> Genetic inactivation of *ABI1* leads to downregulation of WAVE1 and WAVE2 and its complex components, which cannot be compensated by the upregulation of *Abi2* levels. The latter apparently coincides with enhanced levels of WAVE3.<sup>11</sup> Increased levels of WAVE1 and WAVE3 have been linked to invasive prostate cancer in patients,<sup>16,17</sup> indicating the importance of understanding the role of WAVE complexes in human pathology.

Further study of *Abi1*'s tumor suppressive function is warranted given its association with WAVE complexes and the opportunity for the development of new *Abi1*-based therapeutics for the treatment of prostate cancer. Here, we identify the presence of inactivating *ABI1* mutations in archived prostate tumor tissue, thus supporting the hypothesis that *ABI1* loss of heterozygosity has a role in human prostate cancer. To further test this hypothesis, we conditionally disrupted *ABI1* in the mouse prostate. Although some changes could be qualified as hyperplasia, these mice develop prostatic intraepithelial neoplasia (PIN), thus further supporting a tumor suppressor role for *Abi1* in prostate cancer.

## RESULTS

### Exome sequencing identifies mutations in *ABI1* locus

Genomic DNA was obtained from matched (adjacent tissue) normal and prostate tumor-containing tissue microarray samples. Sequencing effort concentrated on analysis of the coding sequence of *ABI1*. *ABI1* exon-containing fragments, obtained by PCR amplification using nested primers derived from flanking introns (Table 1), were sequenced. For each amplified *ABI1* fragment, sequence information was obtained by direct sequencing of PCR fragments and by sequencing subclones of the fragments (Figure 1 and Table 2). We also examined 12 archival cases of matched tumor prostate tissue and normal lymph node biopsies. In this group, *ABI1* mutations were found in prostate tissue, but no DNA changes were found in the lymph biopsies, thus suggesting existence of somatic *ABI1* mutations in prostate cancer. Here, we report 6 recurring *ABI1* mutations in the 35 *ABI1* genes we sequenced.

### Type and location of *ABI1* mutations

Three types of recurring mutations were found: point mutations, that is, single-nucleotide deletions or substitutions, and an exonic deletion owing to intronic mutations. The two cases of intronic

mutations (PT6 and PT7) shared the same 5'-breakpoint mutation site but different 3'-site, but both mutations led to in-frame exon 10 deletions (Figure 1b). Deletion of the nucleotide base 'G' following glycine 331 (G331#) was identified in two tumors, PT25 and PT26. The alanine to serine (A363S) or to aspartic acid (A363D) substitution were found in samples PT21 and mPT2; both mutations are due to single-nucleotide substitutions. All above mutations were only present in the tumor tissues. DNA chromatograms of detected mutations are presented in Figure 1b.

### Consequence of *ABI1* mutations

**Protein truncation.** The deletion following G331 leads to a premature stop codon. This will result in a truncated protein lacking the *Abi1* SH3 domain (Table 2). The SH3 domain is critical for interactions with several actin cytoskeleton regulatory proteins such as N-WASP<sup>18</sup> and mDia.<sup>14</sup> *Abi1* SH3 domain is also a major site for the interaction with c-Abl tyrosine kinase and this interaction was proposed to regulate Abl tyrosine kinase and cell growth negatively.<sup>19</sup> Moreover, the prostate tumor cell line LNCaP carries a mutation in another *Abi1* interaction site for c-Abl, namely deletion of exon 6,<sup>4</sup> which contains tyrosine 213 responsible for high-affinity interaction with Abl SH2 domain and for regulation of Abl kinase activity.<sup>6</sup> Hence, mutations leading to the *Abi1*-lacking SH3 domain or tyrosine 213 raise the possibility of abnormal Abl kinase activity in prostate cancer cases.

**A363D and A363S substitutions.** It remains to be established whether these mutations lead to functional changes in the protein owing to gain of a potential serine phosphorylation site or owing to the occurrence of phosphorylation mimicking aspartic residue. *Abi1* is known to be phosphorylated on serine residues and the pattern of serine phosphorylation has been proposed to be critical for WAVE complex activation<sup>12</sup> downstream from Erk kinase.<sup>20</sup>

**Exon 10 deletions.** Deletion of exon 10, identified in two cases, would lead to the lack of expression of *Abi1* isoforms that contain exon 10, that is, isoforms 1, 2 and 4.<sup>5</sup> The presence of exon 10 in an *Abi1* isoform modulates the Rac1-binding affinity to WAVE2 complexes.<sup>21</sup>

Expression of *Abi1* inhibits cell growth and proliferation of LNCaP cells *in vitro* and in a xenograft model

To test the *Abi1* tumor suppressor hypothesis, we performed complementation assays. For this purpose, we used the relevant human prostate cell line LNCaP, which exhibits low levels of *Abi1* expression<sup>21</sup> owing to the heterozygous exon 6-skipping mutation.<sup>4</sup> We evaluated cell growth, anchorage-independent cell

**Table 1.** List of primers

<i>ABI1</i> exon no.	5' Primer <sup>a</sup>	3' Primer <sup>a</sup>
Exon 1	5'-gggctggagagagtgaggaggaagggga-3'	5'-tggctactcggcggtctct-3'
Exon 1-seq	5'-agagagtgaggaggaaggggaggagtg-3'	5'-gggctggctactcggcggtctct-3'
Exon 2	5'-agtggcccttttagtgagcta-3'	5'-catgcaggctattactcttggc-3'
Exon 3	5'-cctaatatggtccagtgatagtg-3'	5'-aattataatgagcagctgctaaagag-3'
Exon 4	5'-ttctttacaagtagtgaaacatgctgg-3'	5'-ttaacacagccaagctaaatgttg-3'
Exon 5	5'-aaataatggaagcaagtgcaag-3'	5'-tggatccatacacttacttaagtc-3'
Exon 6	5'-ttactcagcacctcataggagt-3'	5'-aaatcctggtatcatggtcaca-3'
Exon 7	5'-ctaattattcagcctccacaataaag-3'	5'-gttttttttaaatatgtctctagaattg-3'
Exon 8	5'-cttcttgctgttcaaatgttgag-3'	5'-agaagccttcaccagaagtagtg-3'
Exon 9	5'-ctgcttgctgctccatcaagtg-3'	5'-tgtctatcatggcaagaataacag-3'
Exon 10	5'-gttcttgcatcactatgttggtg-3'	5'-ggtcagtgccatgcacacaagag-3'
Exon 11	5'-ggattagatgttcttatagttc-3'	5'-gttaactataagttccatcta-3'
Exon 12	5'-atttggatagtgcaactcatgtg-3'	5'-gcataatcagttatggacagctct-3'

<sup>a</sup>Primers for PCR amplification of *ABI1* gene exonic regions were derived from intronic sequences located 5' to (5' primer) or 3' to (3' primer) the indicated *ABI1* exon. The same primers were used for sequencing, except for Exon 1, where Exon 1-seq primers were used.

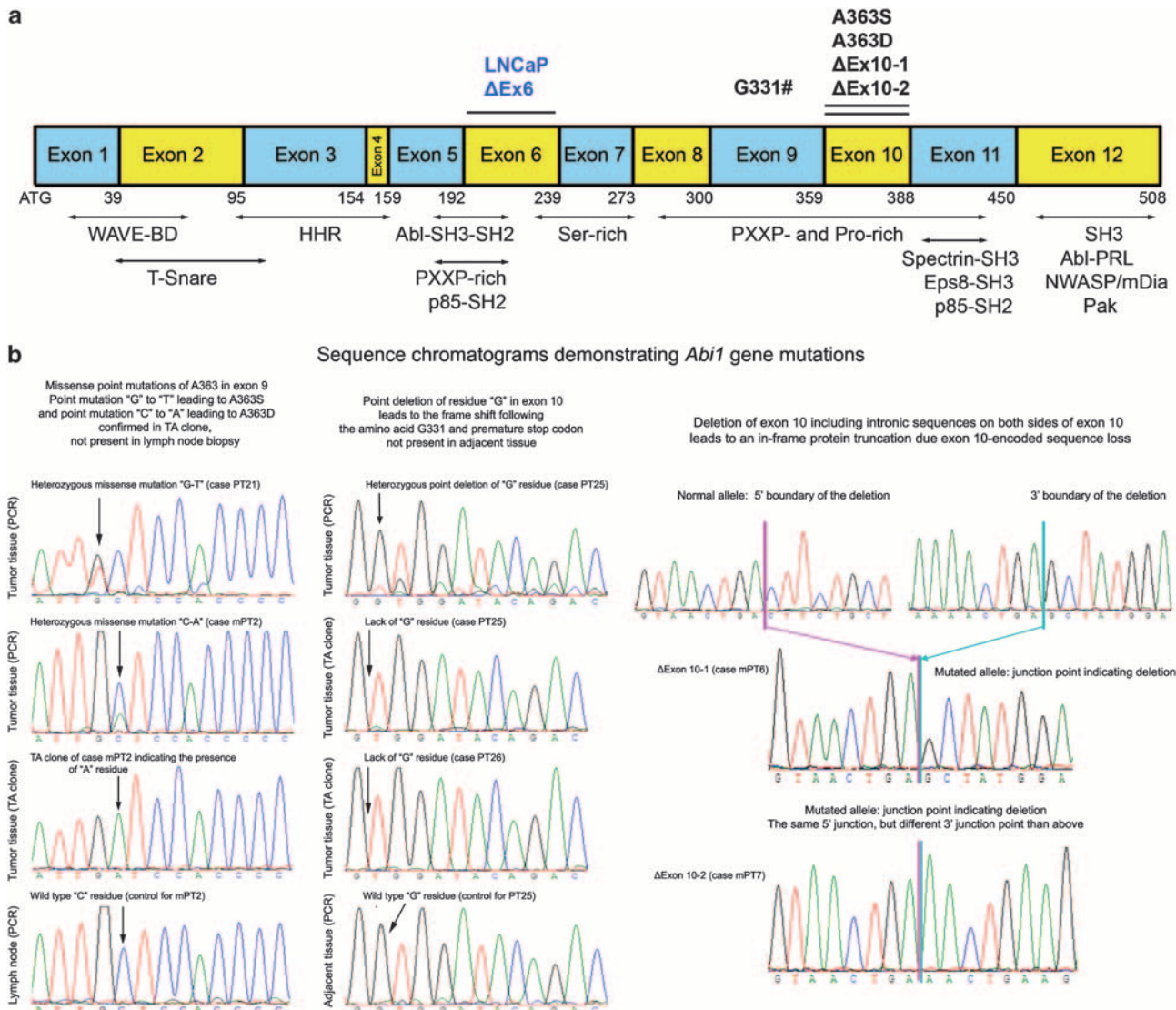


**Figure 1.** Identification of *Abi1* mutations in primary prostate tissue. **(a)** Diagram of *ABI1/SSH3BP1* gene with identified prostate tumor mutations. Boxes indicate coding region of consecutive exons (1–12) as indicated) of *ABI1/SSH3BP1* gene with exonic mutation listed above boxes. Deletions encompassing entire exons (exon 6 and exon 10) are indicated by lines. Numbers below boxes depict the last amino acid encoded by the specific exon or encoded by a shared codon from two consecutive exons. Lines with arrows indicate approximate locations of *Abi1/Hssh3bp1* structural domains and identified binding regions for listed proteins or their domains. WAVE-BD, WAVE domain-binding region;<sup>40,41</sup> HHR, homeo-domain homologous region; Abl-SH3-SH2, c-Abl kinase SH3-SH2 domain-binding region<sup>6</sup> PXXP-, Ser- or Pro-rich, sequences rich in SH3 domain-binding consensus PXXP, serine or proline residues, respectively; SH3, Src homology 3 domain. Indicated binding sites for: Spectrin-SH3, Spectrin Src Homology 3 domain; Eps8-SH3, Eps8 Src Homology 3 domain; p85, p85 regulatory subunit of phosphoinositide-3 kinase; p85-SH2, p85-Src Homology 2 domain; Abl-PRL, c-Abl kinase proline-rich region, N-WASP and mDia. LNCaP Δex6, indicates exon 6 deletion;<sup>4</sup> ATG, start codon. **(b)** DNA sequence chromatograms demonstrating recurring *Abi1* mutations. Chromatograms from tumor tissue and tissue adjacent to tumor or archived lymph node biopsy are shown. The text above chromatograms indicates location and primary consequence of mutations. Left panel demonstrates A363S and A363D mutations; middle panel, deletion following codon G331 (#G331); right panel demonstrates complete deletion of exon 10.

growth and proliferation of stably transfected LNCaP cells that expressed *Abi1* (Figures 2a–c). *Abi1* expression inhibited cell growth (Figure 2a) and proliferation (Figure 2b) in comparison with the mock-transfected cell line. By analyzing the function of a prostate tumor mutant form of *Abi1*-lacking exon 10, *Abi1* ΔEx10, we determined that the mutant failed to inhibit cell proliferation (Figure 2b) or to promote cell-to-cell adhesion in cell aggregation assays (Figure 2c).

We have also compared anchorage-independent growth of LNCaP cells expressing wild-type (wt) *Abi1* vs cells expressing *Abi1*-A363S mutant using soft agar colony formation assay. LNCaP *Abi1* wt cells formed lower number of colonies in comparison with

the mock-transfected control cells. In contrast, expression of *Abi1* A363S mutation failed to suppress colony formation (Figure 2d). In addition, growth of xenograft tumors derived from *Abi1*-transfected LNCaP cells was significantly lower ( $P < 0.05$ ) than tumors derived from mock-transfected cells (Figure 2e). These results support the tumor suppressor function of *Abi1*.

Disruption of *Abi1* expression leads to PIN in mice

To address the tumor suppressor hypothesis *in vivo*, we used a conditional *Abi1* knockout (KO) mouse recently generated in our laboratory.<sup>11</sup> Prostate-specific disruption of *Abi1* expression was

**Table 2.** *ABI1* mutations in primary prostate tumors

Case no.	Location	Nucleotide change	Type of mutation	Amino-acid change	Functional outcome	Tumor grade/stage
PT25	Exon 9	tctg(g/–)tgga	Deletion	G331#	Premature stop codon/lack of SH3 domain	7/2
PT26	Exon 10	tctg(g/–)tgga	Missense	G331#	Unknown/gain of phosphorylation site (pS)?	9/3
PT21		tatt(g→T)ctcc		A363S		8/2
mPT2	Exon 10	attg(c→A)tcca	Deletion	A363D	Loss of exon 10 function	7/3
mPT6		ctga(cttc.del.ctga)gcta		In-frame loss of exon 10		9/3
mPT7		ctga(cttc.del.ctga)aact				7/2

(x/–) indicates deletion of 'x' residue; (x→X) indicates point mutation; and (xxxx.del.xxxx) indicates intronic boundary of exon 10 deletions. PT, microarray cases; mPT, indicates additional samples; and case-matched normal lymph node biopsy did not show these mutations. The last column contains Gleason/TNM score.

obtained by breeding *Abi1* floxed mouse strain (*Abi1* fl/fl) with the probasin promoter-driven Cre strain (*PbCre4*). *PbCre* (+) mice heterozygous for the *Abi1* floxed allele (*Abi1* fl/+)) were bred together to generate *PbCre* (+) *Abi1* (fl/fl) homozygotes. Cre-mediated recombination was confirmed in anterior and dorsal prostate lobes of 24-week-old animals (Figure 3a).

Male mice of specific genotypes and specified ages were evaluated for the presence of primary tumorigenic changes in the prostate and presence of metastatic growth in other tissues. Histopathological evaluation indicated no changes at 4 months but showed the presence of tumorigenic changes at 8 months (Figure 3b). These changes appeared in the form of mouse PIN (mPIN) (Bar Harbor Classification),<sup>22</sup> although some changes could be classified as hyperplasia or atypical PIN (see also below). Changes were present only in dorsal and/or anterior prostates in mice homozygous for *Abi1* floxed alleles with Cre expression (*Abi1* (fl/fl) *PbCre* (+)) at 8 months (Figure 3b). We also observed PIN-like changes in two mice with (*Abi1* (fl/fl) *PbCre* (–)), but not in the control strain at 8 months. Subsequent observations of (*Abi1* (fl/fl) *PbCre* (+)) mice indicated no progression beyond hyperplasia/mPIN (that is, no invasive cancer or metastatic changes were observed at 10 and 12 months). Representative images (HE staining) from *Abi1* KO mouse prostate tissue are shown in Figure 4A.

#### Characteristic features of histopathological changes in *Abi1* KO prostate

Initial changes in the prostate of 8-month-old mice were subtle and characterized by nuclear changes that occurred within a few scattered cells (Figure 4B). Subsequently, a few glands demonstrated nuclear atypia (karyomegaly, prominent nucleoli and hyperchromatic nuclei), with or without cytomegaly (Figure 4B). However, in many areas nuclei remained small, round, regular and homogeneous, with low N/C ratio, which could be qualified as hyperplasia or atypical PIN. More pronounced changes affecting luminal cells in all prostate glands included a piling up of epithelial cells (into two or more layers) and a thickening of acinar folds (Figure 4).

#### Disruption of *Abi1* expression leads to downregulation of WAVE2 complex and cellular adhesion proteins

Previous studies suggested a role for *Abi1* in cell-to-cell adhesion<sup>14</sup> involving the WAVE2 complex.<sup>13</sup> Western blot examination of the prostate tissue from mice with Cre expression demonstrated a decreased amount of *Abi1*, as expected, as well as decreased amounts of WAVE2 and Nap1, which, like *Abi1*, are components of the WAVE2 complex

(Figure 5a). Enhanced *Abi2* expression was observed in prostate tissue lacking *Abi1*, while E-cadherin and  $\beta$ -catenin expression was decreased (Figure 5a). Immunohistochemistry confirmed upregulation of *Abi2* in mPIN regions (Figure 5b, upper panel), and concomitant upregulation of cellular proliferation as indicated by Ki67 staining in these regions (Figure 5b, middle panel). Moreover, the phospho-Akt signal accumulated in PIN lesions (Figure 5b, lower panel). Hence, disruption of *Abi1* in the prostate leads to enhanced cellular proliferation and downregulation of cellular adhesion markers.

To derive a mechanistic explanation for the enhanced cellular proliferation downstream from phospho-Akt, we examined the response to epidermal growth factor treatment of syngeneic *Abi1* KO mouse embryonic fibroblast (MEF) cell lines.<sup>11</sup> Cells lacking *Abi1* showed significant upregulation of phospho-Akt S473, although the response of two independent *Abi1* KO clones demonstrated different dynamics (Figures 6a and b). However, both clones exhibited enhanced colony formation (Figures 6c and d), thus demonstrating the enhanced proliferation phenotype.

## DISCUSSION

We tested the hypothesis that *ABI1* acts as tumor suppressor gene. Identification of mutations in primary prostate tumors from patients, inhibition of cell growth and proliferation of LNCaP cells *in vitro*, inhibition of growth in soft agar assay and inhibition of tumor formation in a xenograft assay all support the hypothesis that *Abi1* acts as a tumor suppressor. Most importantly, recapitulation of histopathological changes in mice upon disruption of *ABI1* reminiscent of PIN provides proof-of-concept evidence for the tumor suppressor function of the gene in the prostate. Given the results of this study, further analysis of the role of *ABI1* in other cancers is warranted.

*Abi1* mutations exist in primary prostate tumors, but the frequency of these mutations remains to be established

We identified three recurring mutation sites in *Abi1* gene, the point deletion in exon 9, single-nucleotide residue-missense substitutions leading to A363S or A363D replacement, and two exon 10 deletions owing to intronic mutations. Intronic *Abi1* mutations were previously identified in prostate tumors.<sup>23,24</sup> More intronic *Abi1* gene mutations are reported in the melanoma, liver and lung cancer ([http://dcc.icgc.org/martreport/?report=report&mart=gene\\_report&ensembl\\_gene\\_id=ENSG00000136754](http://dcc.icgc.org/martreport/?report=report&mart=gene_report&ensembl_gene_id=ENSG00000136754)). Previously, *Abi1* missense mutations were reported in glioblastoma (D433N substitution)<sup>25</sup> and for head and neck cancer (A105T substitution).<sup>26</sup> Further studies are needed to



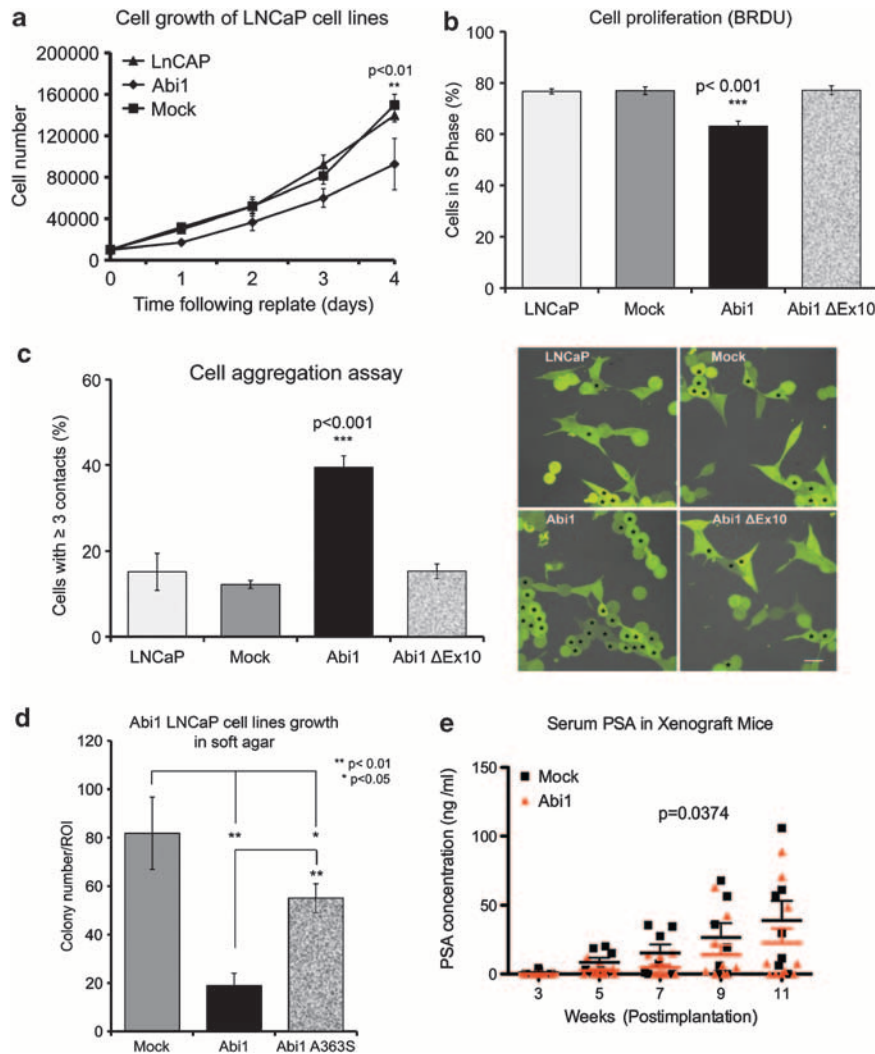


**Figure 2.** Expression of *Abi1* in LNCaP cell line inhibits cellular growth, anchorage-independent growth and proliferation *in vitro* and in xenograft model. **(a)** Inhibition of cell growth, and **(b)** cell proliferation of LNCaP cells expressing *Abi1*. LNCaP cells transfected with *Abi1* proliferate slower than mock-transfected cells. Cell proliferation was evaluated by 5-bromo-2-deoxyuridine incorporation as described in Materials and methods. The data indicate that the percentage of cells in S phase was significantly lower among cells transfected with *Abi1* isoform 2 (*Abi1*) than among cells transfected with isoform 2-lacking exon 10 (*Abi1* ΔEx10), or mock transfected, ( $P < 0.001$ ,  $\chi^2$ ). **(c)** Expression of *Abi1* but not the mutant *Abi1* ΔEx10 promotes cell-to-cell adhesion. Cell aggregation assay was performed as described in Materials and methods. *Left panel*, quantification of cell-to-cell contacts;  $***P < 0.001$ ,  $n = 3$ . *Right panel*, representative images from indicated cell lines: cells with three or more contacts are indicated by asterisks. **(d)** *Abi1* mutant A363S does not inhibit colony formation as well as wt *Abi1*. LNCaP cell lines expressing *Abi1* or *Abi1* containing a known prostate cancer mutation in exon 10 (A363S) were plated in soft agar and evaluated for colony growth 4 weeks later. Numbers of colonies over a defined size ( $> 0.5$  cm in images taken from agar plates) were scored positive and counted per region of interest (ROI),  $n = 3$ . A363S cell line showed enhanced growth vs the *Abi1* isoform 2 expressing cell line,  $**P < 0.01$ ;  $*P < 0.05$ . **(e)** *Abi1* inhibits of tumor growth in LNCaP xenograft assay. Growth of tumors was monitored by prostate-specific antigen (PSA) as described in Materials and methods.<sup>39</sup> Expression of *Abi1* inhibits secretion of serum PSA. Some animals did not develop tumors hence no secretion of PSA was observed. *Abi1*, *Abi1* isoform 2 expressing cell line; mock, cell line expressing empty plasmid. Comparison between the cell lines indicates statistical significance between the groups ( $n = 0.0374$ , two-way analysis of variance).

determine frequency of *Abi1* gene mutations in prostate and other types of human cancer.

*Abi1* exon 10 carries a tumor suppressor function

*Abi1* mutations involving exon 10 failed to reconstitute its tumor suppressor function in LNCaP cells with respect to cellular proliferation. Exon 10 probably has an important role in cell-to-cell adhesion, as the mutant lacking *Abi1* exon 10 did not promote cell-to-cell contacts in cell aggregation assays. Interestingly, exon 10 is naturally lacking from the alternatively spliced *Abi1* isoform 3.<sup>5</sup> Modeling of *Abi1* isoform function in LNCaP cells

indicates that overexpression of isoform 3 leads to enhanced macropinocytosis, enhanced cell spreading and higher active Rac1 levels (active Rac1 also binds to exon 10),<sup>21</sup> which are all features of enhanced tumorigenicity. These data support the hypothesis that *Abi1* exon 10 mutations leading to expression of an isoform 3 mimetic result in a tumorigenic phenotype.

The *Abi1* KO mouse has several characteristics, which make it a desirable model of prostate cancer

For example, nuclear atypia occurs very early in the development of lesions, either slightly before or at the same time as cellular

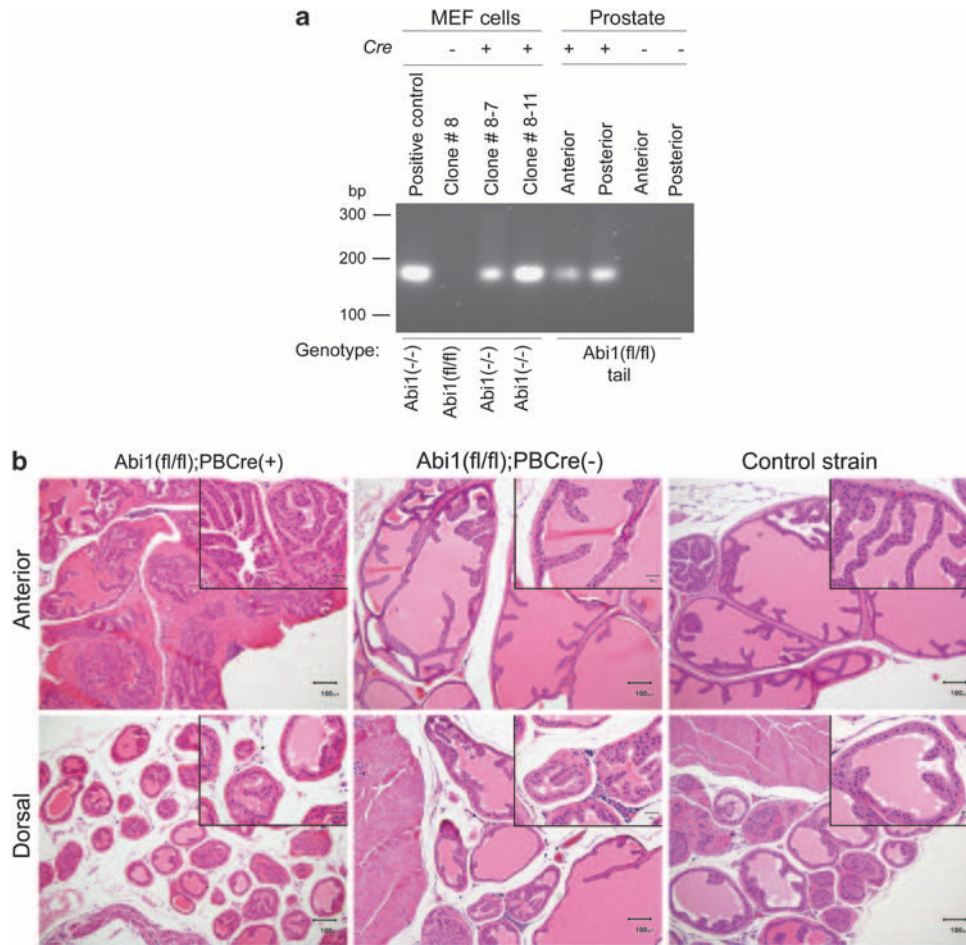


**Figure 3.** The onset of histopathological changes in *Abi1* KO mice at 8 months. **(a)** Confirmation of *Abi1* gene disruption in mouse prostate. DNA was isolated from *Abi1* (fl/fl) mouse prostates (anterior and dorsal lobes) positive for the Cre recombinase-expressing allele (+) or with no Cre presence (-), as shown in the indicated genotypes. PCR using nested primers encompassing the recombined DNA region was carried out as described in Materials and methods. Positive bands were detected only in samples with Cre expression. As controls-immortalized *Abi1* floxed MEF cells were used, parental, that is, of the genotype *Abi1* (fl/fl) or upon Cre-mediated disruption of *Abi1* gene (clone names above the panel). The fidelity of the Cre-mediated recombination was confirmed by DNA sequencing of PCR fragments. **(b)** The earliest time of observation for mPIN in mice-lacking *Abi1*, that is, of the genotype *Abi1*(fl/fl);PBCre(+), is 8 months. Comparison of changes noted in the anterior and dorsal lobes of 8-month-old *Abi1*(fl/fl);PBCre(+) mice vs age-matched Cre (-) and background control strain mice. *Abi1*(fl/fl);PBCre(+) mice feature hyperplasia/mPIN changes, with multiple glands lined by crowded epithelial cells, as well as disorderly piling up of cells in the more severely affected areas. Atypical nuclear changes (best visualized in the inserts), including karyomegaly and hyperchromasia, are also present in many glands. Glands from both the Cre (-) and control strain mice are unremarkable. Number of mice evaluated per genotype at 8 months,  $n > 5$ .

proliferation and atypical growth patterns occur, and without stromal proliferation (that is, lesions are consistent with neoplasia rather than benign prostatic hyperplasia). Although, some areas remain more consistent with hyperplastic lesions, because many nuclei remain small and homogenous, changes more reminiscent of mPIN do occur with advancing age, that is, at 8 months, thus mimicking the development of disease in humans. Although prostate pathology in *Abi1* KO mice has not yet been shown to progress beyond hyperplasia/mPIN, this could occur in older mice (> 12 months of age), and evaluation of older mice is warranted.

Molecular findings indicate that *Abi1* KO prostate has dysregulated cell-to-cell adhesion through downregulation of WAVE2 complex

*Abi1* histopathological changes demonstrated alterations in several proteins critical for cell-to-cell adhesion, most importantly in the levels of E-cadherin and  $\beta$ -catenin. These changes occur most likely downstream from the WAVE2 complex, which is downregulated as a consequence of *Abi1* loss, as these changes

were also recently observed in *Abi1* KO MEF cells.<sup>11</sup> WAVE2 complex has been demonstrated to be important for cellular adhesion in MDCK cells.<sup>13</sup> More recently, it was suggested that WAVE2 complex is important for the formation of initial, 'nascent' cell-to-cell contacts,<sup>14</sup> rather than for maturation of cell-cell junctions.<sup>13</sup> Taken together, these observations suggest that dysregulation of cellular adhesion might explain the appearance of histopathological changes in *Abi1* KO mice. Comprehensive understanding of this process is important from a clinical point of view as targeting cellular adhesion offers therapeutic opportunities in prostate cancer.<sup>27</sup> *Abi1* KO mice provide a unique animal model for mechanistic studies to elucidate how dysregulated cellular adhesion leads to neoplastic changes.

*Abi1* KO mouse provides a model for WAVE complex dysregulation, which is implicated in human cancer

The loss of another WAVE2 complex component, Sra1/CYFIP, is found in a variety of primary epithelial tumors, including the prostate, thus providing further evidence that dysregulated



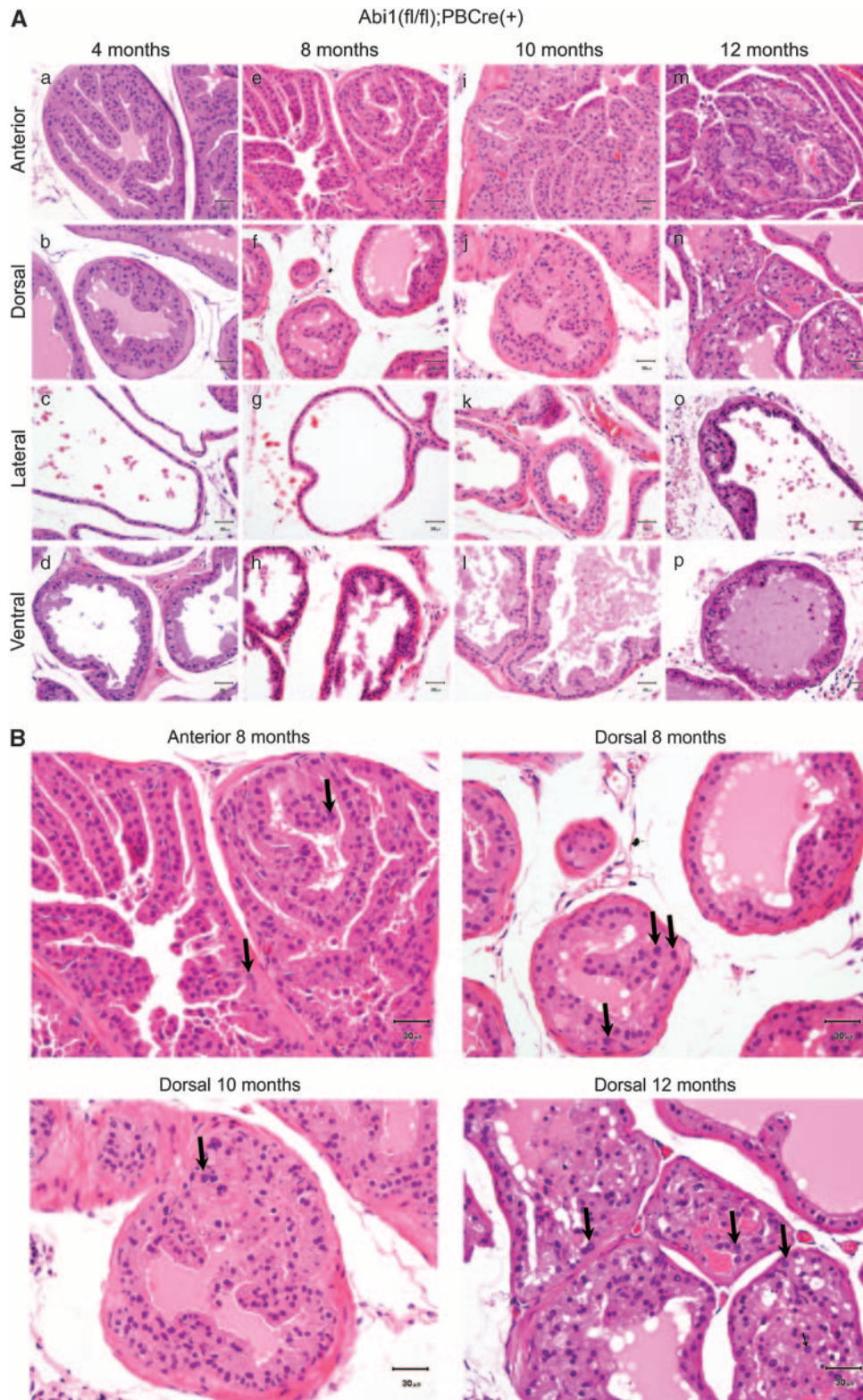


**Figure 4.** Disruption of *Abi1* does not lead to invasive adenocarcinoma in up to 12-month-old mice. **(A)** Summary of observations at 4–12 months of mice lacking both *Abi1* alleles, *Abi1*(fl/fl);PBCre(+). (a–d) At 4 months of age, all prostatic lobes from the *Abi1* KO mice appeared normal. (e–h) At 8 months of age, the anterior (e) and dorsal (f) lobes of *Abi1* KO mice featured multiple gland profiles lined by crowded cells, many of which had enlarged hyperchromatic nuclei. In several affected areas, cells were piled up in a disorderly fashion (consistent with PIN). Lateral (g) and ventral (h) lobes were unremarkable. (i–l) At 10 months of age, a few glands within the lateral (k) lobes are also affected. Ventral (l) lobes are virtually unaffected. (m–p) At 12 months of age, all lobes of *Abi1* KO mice demonstrated some degree of hyperplasia/mPIN changes. These changes were most prominent in the anterior lobe (m), in which the epithelium in the region shown here demonstrated a high degree of cellular atypia. All panels represent hematoxylin and eosin staining (h and e). At least four mice were evaluated per each time point; all mice were positive for histopathological changes at 10 and 12 months. **(B)** Nuclear atypia in *Abi1* KO prostate. Enlarged selected panels from **(A)** to indicate nuclear atypia (arrows).

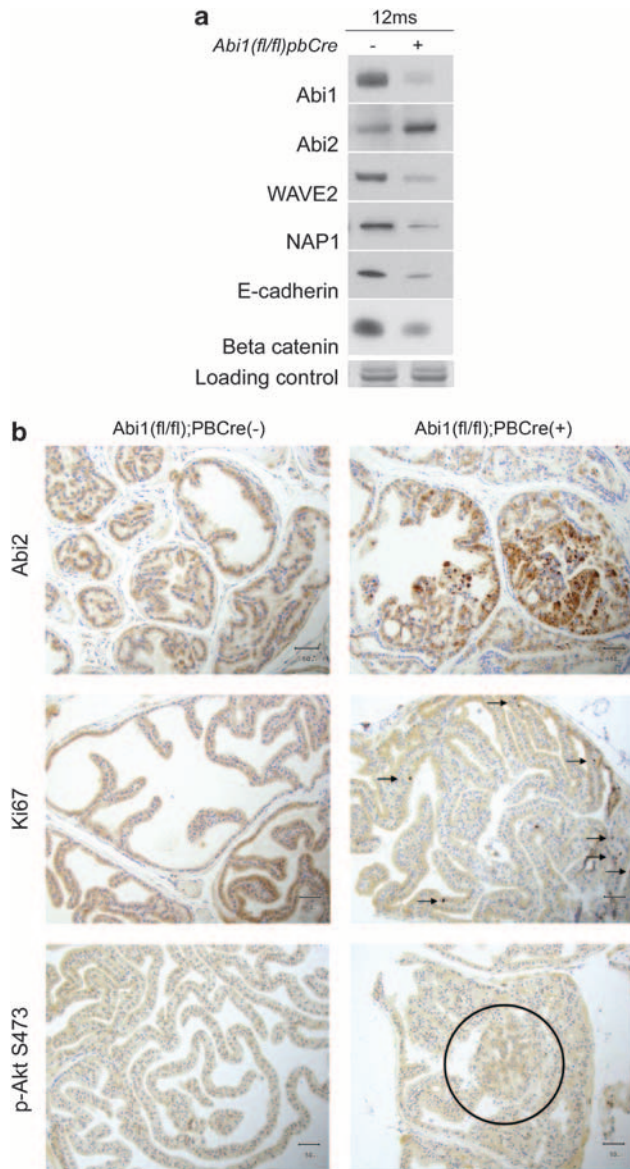


**Figure 5.** Prostate tissue lacking *Abi1* exhibit enhanced proliferation and loss of cellular adhesion markers downstream of WAVE2 complex downregulation. **(a)** Cells and prostate tissues lacking *Abi1* exhibit downregulation of WAVE2 complex components but upregulation of *Abi2* as indicated by western blotting analysis. Examination of WAVE2 complex integral proteins as indicated in *Abi1* KO MEF cells **(a)**; and in prostate tissue **(b)**. Please note coincidental downregulation of E-cadherin in prostate tissue and upregulation of *Abi2* evident at 12 months in *Abi1* KO MEF cells. Anterior prostates were analyzed at 10 and 12 months, ‘-’ indicates absence of probasin Cre recombinase transgene and ‘+’ indicates its presence in *Abi1* floxed mice. **(b)** Enhanced cellular proliferation in prostate tissue lacking *Abi1* correlates with enhanced *Abi2* levels in prostate tissue. Top: immunostaining of *Abi1* KO prostate tissues with *Abi2* antibody. Staining with *Abi2* antibody (P20, Santa Cruz Biotechnology) reveals striking upregulation of *Abi2* levels in *Abi1* KO lesions. Middle: enhanced proliferation as indicated by positive staining with Ki67. Bottom: immunostaining with phospho-Akt S473 antibody indicating staining in the PIN lesion (circle). Right panels, prostate tissue from *Abi1* lacking (*Abi1(f/f);PBCre(+)*); left panels, prostate tissue from with *Abi1* expression (*Abi1(f/f);PBCre(-)*). Staining of tissue was performed as described in Materials and methods.

cellular adhesion resulting from downregulation of WAVE complex has a role in prostate tumorigenesis.<sup>15</sup> Interestingly, *Sra1/CYFIP1* downregulation was linked to increased invasion. As the WAVE complex has a role in cell–matrix adhesion in addition to cell-to-cell adhesion, a combination of the two is likely to be important for epithelial tissue integrity. Interestingly, we have seen no evidence thus far that the loss of *Abi1*, affecting complexes important for cell-to-cell adhesion in the prostate tissue, leads to an invasive phenotype.

Our previous results indicate that increased *Abi2* protein could not compensate for *Abi1* protein loss in WAVE1 or WAVE2 complex integrity in MEF cells. Downregulation of WAVE2 and Nap1 subsequent to *Abi1* inactivation is observed here in the prostate lacking *Abi1*. These data are indicative of lower WAVE2 complex integrity in *Abi1* KO prostate. Interestingly, WAVE3 levels were increased in *Abi1* KO MEF cells.<sup>11</sup> Increased levels of WAVE1<sup>16</sup> and WAVE3<sup>17</sup> complex have been linked to invasive prostate cancer, indicating the importance of analyzing WAVE proteins in future studies involving the *Abi1* KO mouse model.

Loss of *Abi1* leads to abnormal cell growth through dysregulation of the Akt pathway

WAVE complex dysregulation coincides with enhanced cell proliferation as indicated by Ki67 in prostate tissue. Enhanced phospho-Akt levels might be the pathway responsible for the abnormal proliferation as indicated by syngeneic *Abi1* KO cell results. This might occur through dysregulation of PI3 kinase through an abnormal interaction with the p85 regulatory subunit.<sup>7</sup> It is of note that LNCaP cells carry a mutation of the *Abi1*-p85-SH2 C-terminal domain interaction site (Figure 1).<sup>4</sup> Oncogenic mutations involving the p85 C-SH2 domain have been observed in mammalian cancer.<sup>28</sup> Murine lymphomas contain deletions of the C-terminal region comprising the entire C-terminal SH2 domain,<sup>29</sup> human ovarian and colon cancer contain smaller deletions just upstream of the C-SH2 domain.<sup>30</sup> Hence, tumorigenic processes favor negative selection of elements that are critical for cell growth regulation—as demonstrated here, the *Abi1* gene being one of them.

The *Abi1* conditional mouse represents a model for studies of early changes in prostate cancer

The *Abi1* conditional KO mouse provides the first genetic model for evaluation of *Abi1* and WAVE complex involvement in prostate tumorigenesis. Several other mouse models of prostatic adenocarcinoma demonstrating PIN have been developed.<sup>31–33</sup> Examples of the most relevant to the model presented here, that is, conditional models demonstrating PIN upon the target gene disruption, include *Nkx3.1*,<sup>34</sup> *FlIMP*,<sup>35</sup> and  $\beta$ -catenin.<sup>36</sup> Single-copy disruption of *PTEN* also leads to PIN.<sup>37</sup> Studies using these models, as well as the *Abi1* conditional KO model, add to the detailed knowledge about changes in cellular processes implicated in tumorigenesis. Nevertheless, it is apparent that single-gene inactivation in the mouse prostate does not fully recapitulate human disease, which evidently involves numerous genetic aberrations. In this regard, compound genetically altered mice in which two or more genes are conditionally inactivated in the prostate may better model prostate cancer progression.

## MATERIALS AND METHODS

### Prostate tissue

Tissue microarrays were purchased from Telechem International, Inc. (Temecula, CA, USA). The microarray (A302) was constructed using 1.0-mm cores of prostate tumor tissue (arrayed in duplicate) and case-matched normal prostate tissue from 23 cases. The cases were annotated with tumor grade and stage. Cores of tumor and normal tissue were available from the same cases for DNA extraction. An additional 12 cases of archived



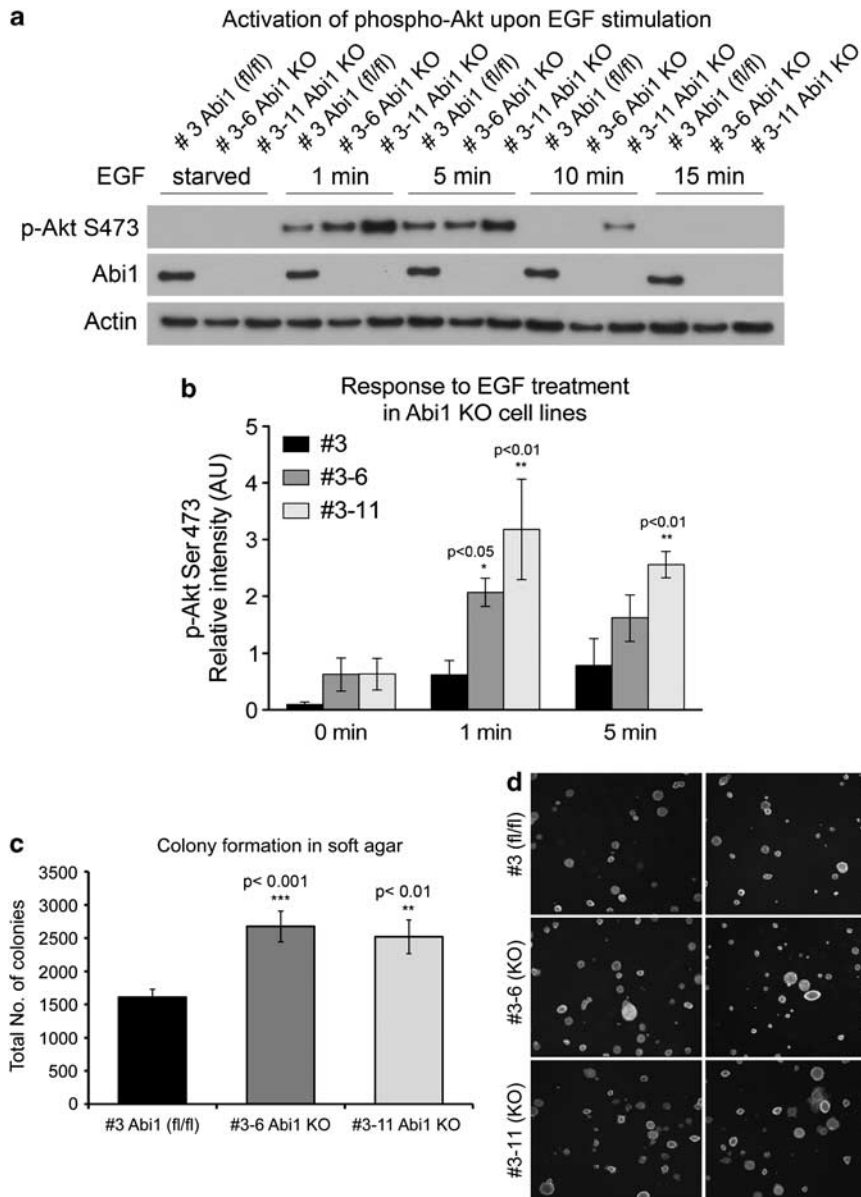


**Figure 6.** Enhanced activation of Akt and colony formation of cells lacking *Abi1*. **(a, b)** MEF cells lacking *Abi1* exhibit enhanced sensitivity to activation of phospho-Akt downstream from EGFR receptor. Cells were starved overnight and subsequently incubated with epidermal growth factor (10 ng/ml) for indicated amounts of time. **(a)** Cell lysates were prepared as described in Materials and methods, and proteins were analyzed by western blotting with indicated antibodies. **(b)** Quantification of phospho-Akt S473 levels indicate significant increase of p-Akt S473 signal of the *Abi1* KO clone #3-11 at 1 min and 5 min ( $P < 0.01$ , two-way analysis of variance); clone #3-6 demonstrated enhanced response vs control #3 cell line at 1 min ( $P < 0.05$ , *t*-test). **(c, d)** Disruption of *Abi1* expression promotes colony formation in soft agar. Syngeneic MEF cells containing or lacking *Abi1* were incubated in soft agar as indicated in Materials and methods, and total numbers of colonies were scored. Cell lines lacking the *Abi1* gene exhibit enhanced colony formation ( $P < 0.001$ , #3-6; and  $P < 0.01$ , #3-11) vs control cell line #3 **(c)**. Representative images of soft agar colonies from two independent experiments **(d)**. #3 represents *Abi1* floxed cell line; #3-6 and #3-11 represent *Abi1* KO cell lines.

tissue of tumor prostate tissue and patient-matched normal lymph node were obtained and analyzed by DNA sequencing.

#### DNA extraction and amplification

Genomic DNA extraction protocol for formaldehyde-fixed-paraffin-embedded (FFPE) tissue was used (QiaAmp DNA Micro Kit, Cat. No. 56304; Qiagen, Valencia, CA, USA) according to the manufacturer's instructions. DNA concentration was determined by PicoGreen fluorescence assay (Cat. No. P7589; Molecular Probes; Eugene, OR, USA). Owing to low yield, DNA obtained from the FFPE samples was amplified using

whole-genome amplification (WGA) kit (Cat. No. WGA5; Sigma-Aldrich, St Louis, MO, USA). The amplification was carried out according to the manufacturer's instructions using Jumpstart Taq polymerase (Cat. No. D9307; Sigma-Aldrich). Amplified DNA was purified using GeneElute PCR purification columns (Cat. No. NA1020; Qiagen) and final DNA concentration was determined as above, or by spectrophotometry.

#### PCR amplification of *AB11* gene exon-containing regions

WGA-amplified genomic DNA obtained from FFPE was amplified by PCR in a final reaction volume of 50  $\mu$ l; containing 5  $\mu$ l of  $10 \times$  HF 2 PCR

buffer, 5  $\mu$ l 10  $\times$  HF 2 dNTP mix, 1  $\mu$ l 50  $\times$  HF 2 polymerase and 2  $\mu$ l of extracted DNA (50–100 ng) and intron-specific Abi1 exon-flanking primers (Table 1). PCR was performed under conditions of an initial denaturation at 94 °C for 2 min, 30–40 cycles consisted of denaturation (30 s at 94 °C), annealing (30 s at 51–58 °C, depending on the primer) and elongation step (30 s at 72 °C), and a final extension step at 72 °C for 7 min. Reactions were performed in a Peltier Thermocycler-DYAD (Bio-Rad Laboratories, Hercules, CA, USA). Each PCR batch included a blank with no DNA. PCR products were visualized in ethidium bromide-stained 1% agarose gel and purified by QIAquick PCR purification kit (Cat. No. 28106; Qiagen), and sense and antisense sequences were obtained by using forward and reverse internal primers, respectively. Sequencing was performed in an ABI PRISM3100 DNA Sequencer (Applied Biosystems, Foster City, CA, USA). All mutations were confirmed from two independent PCR amplifications and from transactivating subclones of PCR products (Cat. No. K4500-40; Invitrogen, Carlsbad, CA, USA). Comparative DNA sequence analysis was performed (Vector NTI Suite, Invitrogen) from tumor and adjacent tissues, and from normal lymph node tissues whenever available.

### Mouse breeding and histopathology

All animal work was performed under the institutional IACUC-approved protocol. Abi1 floxed strain, Abi1(f1/f1), was generated in our laboratory, Abi1<sup>tm1.2Lko</sup> MGI: 4950558.<sup>11</sup> Prostate-specific deletion of Abi1 was obtained by breeding of Abi1 floxed strain (129S:C57BL/6 background) with the mouse strain expressing probasin promoter-driven Cre recombinase, B6.D2-Tg(Pbsn-Cre)4Prb (National Cancer Institute-Frederick; the Mouse Repository of the Mouse Models of Human Cancers Consortium). Upon genotyping (Transnetyx, Cordova, TN, USA), male mice were housed for observations under the designated time schedule. Dissection of prostates and histopathologic evaluation of prostate tissue was performed according to guidelines established for genetically engineered mice (Bar Harbor Classification).<sup>22</sup> The prostate from each mouse was dissected into individual lobes to ensure maximum visualization, and histopathologic analysis was performed on all lobes. Formalin-fixed, paraffin-embedded 5- $\mu$ m tissue sections were processed routinely and stained with hematoxylin and eosin. Each lobe was evaluated and scored for the degree of nuclear and cellular changes.

### Immunohistochemistry

Paraffin sections were dewaxed in xylene and hydrated in graded alcohols. Endogenous peroxidase activity was blocked by immersing the slides in 1% hydrogen peroxide in phosphate-buffered saline for 15 min. Pre-treatment was performed in a pressure cooker using 10 mM citrate buffer, Ph 6.0. Tissue sections were incubated overnight with the following antibodies: Abi-2 (p-20, #sc-203327, Santa Cruz Biotechnology, Santa Cruz, CA, USA, 1:250) and Ki67 (VP-K451, Vector Laboratories, Burlingame, CA, USA, 1:5000). Sections were washed with phosphate-buffered saline and incubated with the appropriate secondary antibodies followed by Avidin–Biotin complexes (Vector Laboratories). Antibody reaction was visualized with 3-3' diaminobenzidine (Sigma-Aldrich) and counterstained with hematoxylin. Tissue sections were dehydrated in graded alcohols, cleared in xylene and mounted.

### Prostate tissue protein extraction and western blot analysis

Anterior prostates were separated from complete prostates at specified ages. Hundred microliter of lysis buffer per 2.5 mg of tissue was used. Samples were homogenized in B-PER-based lysis buffer (B-PER reagent (Pierce Biotechnology, Inc., Rockford, IL, USA), DNase I, protease inhibitor cocktail Set III ethylenediaminetetraacetic acid free, 1 mM Na<sub>3</sub>VO<sub>4</sub>, 1 mM Na<sub>4</sub>P<sub>2</sub>O<sub>7</sub> and 10 mM NaF) by pipetting up and down until homogenous, incubated at room temperature for 10 min, followed by 20 min on ice. Samples were centrifuged at 10 000 *g*, 4 °C for 10 min. The protein concentration in supernatant was quantified by using a Precision Red Advanced Protein Assay Reagent (Cytoskeleton Inc., Denver, CO, USA). Proteins were separated on a western blotting system (Invitrogen) loading no more than 15  $\mu$ g of total protein per lane.

### Immunoblotting

For evaluating protein levels, the following antibodies were used: Abi1 (clone 1B9, MBL International, Woburn, MA, USA); Abi2 (p-20, #sc-20327, Santa Cruz Biotechnology); E-Cadherin (Cat. No. 4065) and phospho-Akt

S473 (Cat. No. #9271) (Cell Signaling Technology, Inc., Danvers, MA, USA); B-catenin (Cat. No. 610154, BD Biosciences, San Jose, CA, USA); Ki-67 (Cat. No. VP-K451, Vector Laboratories); WAVE2 (H-110, #sc-33548; #07-410, Santa Cruz Biotechnology; rabbit polyclonal (#1735) and NAP1 were kind gifts from Theresia Stradal).<sup>11</sup> Secondary horseradish peroxidase-labeled rabbit anti-goat IgG was from Thermo Fisher Scientific Inc., Waltham, MA, USA; goat anti-rabbit IgG was from Cell Signaling Technology and goat anti-mouse was from Jackson ImmunoResearch Laboratories, Inc., West Grove, PA, USA. Coomassie-stained gel, and immunoblotting with the antibody to actin or Rac1 (Cytoskeleton Inc.) were used as loading control in the experiments. Levels of phospho-Akt S473 in Abi1 KO cells lines following epidermal growth factor treatment (10 ng/ml; Sigma-Aldrich) were quantified using ImageJ software (NIH ImageJ), software Version 1.41n). Abi1 KO cell lines, #3-6 and #3-11, and control floxed cell line #3 were cultured as described.<sup>11</sup>

### Growth, soft agar colony formation and proliferation assays

LNCAp cells stably expressing Abi1 were described previously.<sup>7,21</sup> Abi1 A363S site-directed mutagenesis was performed in accordance to the manufacturer's instructions (Stratagene, La Jolla, CA, USA). Stable cell line was established as described previously.<sup>7,21</sup> Rates of cell growth (Abi1 isoform 2) were evaluated by counting the number of cells using BD FACSCanto Flow Cytometer and Flow-Count Fluorospheres Cat. No 7547053-200 as standard (BD Biosciences). Cell proliferation was evaluated using a FITC BrdU Flow Assay, BD Biosciences-Pharmingen, San Diego, CA, USA, BrdU Flow Kit (Cat. No.559619), according to the manufacturer's protocol. The percentage of cells in S phase was determined using flow cytometry. Percentage of cells in S phase was compared between the groups ( $P < 0.001$ ,  $\chi^2$ ). In the soft agar colony formation assay, LNCAp cell lines expressing Abi1-wt or Abi1-A363S prostate cancer mutation were plated in semisolid soft agar-containing RPMI medium and evaluated for colony growth 4 weeks later. At least 10 images were taken per soft agar plate per cell line. Cell lines were plated on the plates in quadruplicates. Number of colonies over a defined size (>0.5 cm in images taken from agar plates) was scored positive and counted per region of interest,  $n = 3$ . The total numbers of soft agar colonies were scored for syngeneic MEF cell lines lacking Abi1 expression following a 4-week incubation.

### Cell aggregation assay

LNCAp cells were replated from confluent plates following trypsin and ethylenediaminetetraacetic acid treatment. Following dissociation into a single-cell suspension, cells were incubated for 5 min in full culture medium and seeded onto collagen-coated 8-chamber culture slides (BD Biosciences) for 4 h, and then evaluated. The cell-to-cell adhesive property of cells was scored as the ability of a cell to form three or more cell-to-cell contacts (50 cells per sample,  $n = 3$ ). Observations were carried out using a Zeiss 510 META confocal microscope (Carl Zeiss Microscopy, LLC, Thornwood, NY, USA). Before replating, cells were labeled with Cell Tracker Green CMFDA according to the manufacturer's protocol (Invitrogen, cat#C2925). LNCAp cell lines expressing Abi1 isoform 2 (Abi1), Abi1 isoform 2-lacking exon 10 (Abi1  $\Delta$ Ex10) and mock-transfected clones were evaluated. The mutant Abi1  $\Delta$ Ex10 in the context of Abi1 isoform 2 is identical to Abi1 isoform 3.<sup>21</sup>

### Xenograft of LNCAp cell lines

Male Swiss Nude mice (NSWNU-M, Taconic Farms Inc., Hudson, NY, USA) (8–10-week-old) were implanted orthotopically with LNCAp cells expressing recombinant Abi1, Abi1-wt (isoform 2) ( $n = 10$ ) or with cells stably transfected with control plasmid, mock ( $n = 9$ ). Tumor growth was monitored by evaluation of serum prostate-specific antigen.<sup>38,39</sup> Tumor burden was monitored in accordance with the institutional and NIH guidelines.

### Statistical analysis

One-way analysis of variance (Figure 2a), two-way analysis of variance (Figures 2e and 6b),  $\chi^2$  (Figure 2b) and Student's *t*-test (Figures 2c, d and 6c) were used for analyses. *P*-values < 0.05 were considered significant and are indicated on graphs as (\*),  $P < 0.01$ (\*\*) and  $P < 0.001$ (\*\*\*). Error bars represent the s.e.m.

### CONFLICT OF INTEREST

Abi1/hSSH3BP1 conditional KO mouse is the subject of a NYBC patent application.

## ACKNOWLEDGEMENTS

We thank the late William Gerald for helpful discussions; Maria Socorro Jiao, Memorial Sloan Kettering Cancer Center, for assistance with tissue immunohistochemistry; and Samit Bhoval for assistance with soft agar assay. This work was supported by grants from the Department of Defense Prostate Cancer Research Program (W81XWH-08-1-0320) (LK) and in part by the NIH R01 NS044968 (LK). Support by the FM Kirby Foundation Inc., Morristown, NJ, USA (LK) is acknowledged.

## REFERENCES

- 1 Yu W, Sun X, Clough N, Cobos E, Tao Y, Dai Z. Abi1 gene silencing by short hairpin RNA impairs Bcr-Abl-induced cell adhesion and migration *in vitro* and leukemogenesis *in vivo*. *Carcinogenesis* 2008; **29**: 1717–1724.
- 2 Wang C, Tran-Thanh D, Moreno JC, Cawthorn TR, Jacks LM, Wang DY *et al*. Expression of Abl interactor 1 and its prognostic significance in breast cancer: a tissue-array-based investigation. *Breast Cancer Res Treat* 2011; **129**: 373–386.
- 3 Cui M, Yu W, Dong J, Chen J, Zhang X, Liu Y. Downregulation of ABI1 expression affects the progression and prognosis of human gastric carcinoma. *Med Oncol* 2010; **27**: 632–639.
- 4 Macoska JA, Xu J, Ziemnicka D, Schwab TS, Rubin MA, Kotula L. Loss of expression of human spectrin src homology domain binding protein 1 is associated with 10p loss in human prostatic adenocarcinoma. *Neoplasia* 2001; **3**: 99–104.
- 5 Ziemnicka-Kotula D, Xu J, Gu H, Potempska A, Kim KS, Jenkins EC *et al*. Identification of a candidate human spectrin Src homology 3 domain-binding protein suggests a general mechanism of association of tyrosine kinases with the spectrin-based membrane skeleton. *J Biol Chem* 1998; **273**: 13681–13692.
- 6 Xiong X, Cui P, Hossain S, Xu R, Warner B, Guo X *et al*. Allosteric inhibition of the nonMyristoylated c-Abl tyrosine kinase by phosphopeptides derived from Abi1/Hssh3bp1. *Biochimica et Biophysica Acta* 2008; **1783**: 737–747.
- 7 Dubielecka PM, Machida K, Xiong X, Hossain S, Ogiue-Ikeda M, Carrera AC *et al*. Abi1/Hssh3bp1 pY213 links Abl kinase signaling to p85 regulatory subunit of PI-3 kinase in regulation of macropinocytosis in LNCaP cells. *FEBS Lett* 2010; **584**: 3279–3286.
- 8 Jia S, Roberts TM, Zhao JJ. Should individual PI3 kinase isoforms be targeted in cancer? *Curr Opin Cell Biol* 2009; **21**: 199–208.
- 9 Eden S, Rohatgi R, AV Podtelejnikov, Mann M, Kirschner MW. Mechanism of regulation of WAVE1-induced actin nucleation by Rac1 and Nck. *Nature* 2002; **418**: 790–793.
- 10 Stradal TE, Rottner K, Disanza A, Confalonieri S, Innocenti M, Scita G. Regulation of actin dynamics by WASP and WAVE family proteins. *Tr Cell Biol* 2004; **14**: 303–311.
- 11 Dubielecka PM, Ladwein Kl, Xiong X, Migeotte I, Chorzalska A, Anderson KV *et al*. Essential role for Abi1 in embryonic survival and WAVE2 complex integrity. *Proc Natl Acad Sci USA* 2011; **108**: 7022–7027.
- 12 Lebensohn AM, Kirschner MW. Activation of the WAVE complex by coincident signals controls actin assembly. *Mol Cell* 2009; **36**: 512–524.
- 13 Yamazaki D, Oikawa T, Takenawa T. Rac-WAVE-mediated actin reorganization is required for organization and maintenance of cell-cell adhesion. *J Cell Sci* 2007; **120**(Pt 1): 86–100.
- 14 Ryu JR, Echarri A, Li R, Pendergast AM. Regulation of cell-cell adhesion by Abi/Diaphanous complexes. *Mol Cell Biol* 2009; **29**: 1735–1748.
- 15 Silva JM, Ezhkova E, Silva J, Heart S, Castillo M, Campos Y *et al*. Cyfip1 is a putative invasion suppressor in epithelial cancers. *Cell* 2009; **137**: 1047–1061.
- 16 Fernando HS, Sanders AJ, Kynaston HG, Jiang WG. WAVE1 is associated with invasiveness and growth of prostate cancer cells. *J Urol* 2008; **180**: 1515–1521.
- 17 Fernando HS, Sanders AJ, Kynaston HG, Jiang WG. WAVE3 is associated with invasiveness in prostate cancer cells. *Urol Oncol* 2010; **28**: 320–327.
- 18 Innocenti M, Gerboth S, Rottner K, Lai FP, Hertzog M, Stradal TE *et al*. Abi1 regulates the activity of N-WASP and WAVE in distinct actin-based processes. *Nat Cell Biol* 2005; **7**: 969–976.
- 19 Dai Z, Pendergast AM. Abi-2 a novel SH3-containing protein interacts with the c-Abl tyrosine kinase and modulates c-Abl transforming activity. *Genes Dev* 1995; **9**: 2569–2582.
- 20 Mendoza MC, Er EE, Zhang W, Ballif BA, Elliott HL, Danuser G *et al*. ERK-MAPK drives lamellipodia protrusion by activating the WAVE2 regulatory complex. *Mol Cell* 2011; **41**: 661–671.
- 21 Dubielecka PM, Cui P, Xiong X, Hossain S, Heck S, Angelov L *et al*. Differential regulation of macropinocytosis by Abi1/Hssh3bp1 isoforms. *PLoS One* 2010; **5**: e10430.
- 22 Shappell SB, Thomas GV, Roberts RL, Herbert R, Ittmann MM, Rubin MA *et al*. Prostate pathology of genetically engineered mice: definitions and classification. The consensus report from the Bar Harbor meeting of the Mouse Models of Human Cancer Consortium Prostate Pathology Committee. *Cancer Res* 2004; **64**: 2270–2305.
- 23 Berger MF, Lawrence MS, Demicheli F, Drier Y, Cibulskis K, Sivachenko AY *et al*. The genomic complexity of primary human prostate cancer. *Nature* 2011; **470**: 214–220.
- 24 Kumar A, White TA, MacKenzie AP, Clegg N, Lee C, Dumpit RF *et al*. Exome sequencing identifies a spectrum of mutation frequencies in advanced and lethal prostate cancers. *Proc Natl Acad Sci USA* 2011; **108**: 17087–17092.
- 25 McLendon R, Friedman A, Bigner D, Van Meir EG, Brat DJ, Mastrogiannis GM *et al*. Comprehensive genomic characterization defines human glioblastoma genes and core pathways. *Nature* 2008; **455**: 1061–1068.
- 26 Stransky N, Egloff AM, Tward AD, Kostic AD, Cibulskis K, Sivachenko A *et al*. The mutational landscape of head and neck squamous cell carcinoma. *Science* 2011; **333**: 1157–1160.
- 27 Tanaka H, Kono E, Tran CP, Miyazaki H, Yamashiro J, Shimomura T *et al*. Monoclonal antibody targeting of N-cadherin inhibits prostate cancer growth, metastasis and castration resistance. *Nat Med* 2010; **16**: 1414–1420.
- 28 Luo J, Cantley LC. The negative regulation of phosphoinositide 3-kinase signaling by p85 and its implication in cancer. *Cell Cycle* 2005; **4**: 1309–1312.
- 29 Jimenez C, Jones DR, Rodriguez-Viciana P, Gonzalez-Garcia A, Leonardo E, Wennstrom S *et al*. Identification and characterization of a new oncogene derived from the regulatory subunit of phosphoinositide 3-kinase. *EMBO J* 1998; **17**: 743–753.
- 30 Philp AJ, Campbell IG, Leet C, Vincan E, Rockman SP, Whitehead RH *et al*. The phosphatidylinositol 3'-kinase p85alpha gene is an oncogene in human ovarian and colon tumors. *Cancer Res* 2001; **61**: 7426–7429.
- 31 Wang F. Modeling human prostate cancer in genetically engineered mice. *Prog Mol Biol Trans Sci* 2011; **100**: 1–49.
- 32 Abate-Shen C. A new generation of mouse models of cancer for translational research. *Clin Cancer Res* 2006; **12**: 5274–5276.
- 33 Kasper S. Survey of genetically engineered mouse models for prostate cancer: analyzing the molecular basis of prostate cancer development, progression, and metastasis. *J Cell Biochem* 2005; **94**: 279–297.
- 34 Abdulkadir SA, Magee JA, Peters TJ, Kaleem Z, Naughton CK, Humphrey PA *et al*. Conditional loss of Nkx3.1 in adult mice induces prostatic intraepithelial neoplasia. *Mol Cell Biol* 2002; **22**: 1495–1503.
- 35 Kelavkar UP, Parwani AV, Shappell SB, Martin WD. Conditional expression of human 15-lipoxygenase-1 in mouse prostate induces prostatic intraepithelial neoplasia: the FLIMP mouse model. *Neoplasia* 2006; **8**: 510–522.
- 36 Pearson HB, Phesse TJ, AR Clarke. K-ras and Wnt signaling synergize to accelerate prostate tumorigenesis in the mouse. *Cancer Res* 2009; **69**: 94–101.
- 37 Trotman LC, Niki M, Dotan ZA, Koutcher JA, Di Cristofano A, Xiao A *et al*. Pten dose dictates cancer progression in the prostate. *PLoS Biol* 2003; **1**: E59.
- 38 Stephenson RA, Dinney CP, Gohji K, Ordonez NG, Killion JJ, Fidler IJ. Metastatic model for human prostate cancer using orthotopic implantation in nude mice. *J Natl Cancer Inst* 1992; **84**: 951–957.
- 39 Garzotto M, Haimovitz-Friedman A, Liao WC, White-Jones M, Huryk R, Heston WD *et al*. Reversal of radiation resistance in LNCaP cells by targeting apoptosis through ceramide synthase. *Cancer Res* 1999; **59**: 5194–5201.
- 40 Leng Y, Zhang J, Badour K, Arpaia E, Freeman S, Cheung P *et al*. Abelson-interactor-1 promotes WAVE2 membrane translocation and Abelson-mediated tyrosine phosphorylation required for WAVE2 activation. *Proc Natl Acad Sci USA* 2005; **102**: 1098–1103.
- 41 Echarri A, Lai MJ, Robinson MR, Pendergast AM. Abl interactor 1 (Abi-1) wave-binding and SNARE domains regulate its nucleocytoplasmic shuttling, lamellipodium localization, and wave-1 levels. *Mol Cell Biol* 2004; **24**: 4979–4993.



Oncogenesis is an open-access journal published by Nature Publishing Group. This work is licensed under the Creative Commons Attribution-NonCommercial-Share Alike 3.0 Unported License. To view a copy of this license, visit <http://creativecommons.org/licenses/by-nc-sa/3.0/>